Maintaining energy homeostasis is an essential component of *Wld^S*-mediated axon protection

Hua Shen [a,*], Krzysztof L. Hyrc [a,b], Mark P. Goldberg [a,1]

[a] Hope Center for Neurological Disorders and Department of Neurology, Washington University School of Medicine, 660 S. Euclid Avenue, Saint Louis, MO 63110, USA
[b] Alafi Neuroimaging Laboratory, Washington University School of Medicine, 660 S. Euclid Avenue, Saint Louis, MO 63110, USA

ARTICLE INFO

ABSTRACT

Wld^S mutation protects axons from degeneration in diverse experimental models of neurological disorders, suggesting that the mutation might act on a key step shared by different axon degeneration pathways. Here we test the hypothesis that *Wld^S* protects axons by preventing energy deficiency commonly encountered in many diseases. We subjected compartmentally cultured, mouse cortical axons to energy deprivation with 6 mM azide and zero glucose. In wild-type (WT) culture, the treatment, which reduced axon ATP level ($[ATP]_{axon}$) by 65%, caused immediate axon depolarization followed by gradual free calcium accumulation and subsequent irreversible axon damage. The calcium accumulation resulted from calcium influx partially via L-type voltage-gated calcium channel (L-VGCC). Blocking L-VGCC with nimodipine reduced calcium accumulation and protected axons. Without altering baseline $[ATP]_{axon}$, the presence of *Wld^S* mutation significantly reduced the axon ATP loss and depolarization, restrained the subsequent calcium accumulation, and protected axons against energy deprivation. *Wld^S* neurons possessed higher than normal nicotinamide mononucleotide adenylyltransferase (NMNAT) activity. The intrinsic *Wld^S* NMNAT activity was required for the *Wld^S*-mediated energy preservation and axon protection during but not prior to energy deprivation. NMNAT catalyzes the reversible reaction that produces nicotinamide adenine dinucleotide (NAD) from nicotinamide mononucleotide (NMN). Interestingly, preventing the production of NAD from NMN with FK866 increased $[ATP]_{axon}$ and protected axons from energy deprivation. These results indicate that the *Wld^S* mutation depends on its intrinsic *Wld^S* NMNAT activity and the subsequent increase in axon ATP but not NAD to protect axons, implicating a novel role of *Wld^S* NMNAT in axon bioenergetics and protection.

© 2013 Elsevier Inc. All rights reserved.

Introduction

Axon degeneration occurs in many neurological disorders and leads to varied degrees of disability. The spontaneous *Wld^S* mutation that delays Wallerian degeneration after nerve injury (Lunn et al., 1989) protects axons in a variety of experimental models of neurological disorders such as multiple sclerosis (Kaneko et al., 2006), Parkinson's

disease (Hasbani and O'Malley, 2006; Sajadi et al., 2004), stroke (Gillingwater et al., 2004; Ryu et al., 2006), traumatic brain and spinal cord injury (Adalbert et al., 2006; Gillingwater et al., 2006), and motor neuron disease (Ferri et al., 2003). Understanding the mechanisms of *Wld^S*-mediated axon protection may reveal invaluable insights into the mechanism of axon injury and provide a basis for new treatments for neurological disorders associated with axon degeneration.

The *Wld^S* mutation is a spontaneous 85-kb tandem triplication (Coleman et al., 1998), which encodes a chimeric protein composed of the N-terminal 70 amino acids of ubiquitination factor Ube4b, a short junction sequence, and the full length of nicotinamide mononucleotide adenylyltransferase 1 (NMNAT1; Mack et al., 2001). NMNAT catalyzes the reversible reaction that produces nicotinamide adenine dinucleotide (NAD) and pyrophosphate (PPi) from ATP and nicotinamide mononucleotide (NMN) in the forward mode or creates ATP and NMN from NAD and PPi in the reverse mode (Lau et al., 2009).

There is compelling evidence indicating that NMNAT activity is required for *Wld^S*-mediated axon protection (Araki et al., 2004; Avery et al., 2009; Conforti et al., 2009; Yahata et al., 2009). NAD, the product of NMNAT forward reaction, as well as many components in the NAD biosynthetic pathway have also been reported to be axon-protective (Sasaki et al., 2006; Wang et al., 2005). These findings have led to a

hypothesis that NAD is the axon survival factor provided by Wld^S via NMNAT. However, this hypothesis is at odds with the observations that neither Wld^S nor NMNAT1 increases steady-state NAD level (Araki et al., 2004; Mack et al., 2001; Wang et al., 2005). Furthermore, a recent study demonstrated that NMNAT activity per se rather than higher NAD level is required for NMNAT-mediated protection (Sasaki et al., 2009). Thus, other mechanisms may be involved in Wld^S/NMNAT-mediated axon protection.

Axon degeneration is often accompanied by energy shortage due to mitochondrial dysfunction, substrate restriction/deprivation, and/or excessive energy consumption (Coleman, 2005; Mattson and Liu, 2002; Stys, 2005; Waxman, 2006). We have shown that reducing axon ATP by over 60% is sufficient to induce irreversible axon damage (Shen and Goldberg, 2012). Interestingly, in addition to protecting axons, Wld^S has also been shown to attenuate axon ATP loss following different insults (Ikegami and Koike, 2003; Wang et al., 2005), suggesting that the ability of Wld^S to sustain axon energy balance might be responsible for axon protection provided by the mutation. To test this hypothesis, we evaluated the effects of Wld^S on axon injury in cultured cortical axons exposed to acute energy deprivation and explored the possible mechanisms of Wld^S-mediated axon protection. Our data support the idea that Wld^S might protect axons by maintaining axon energy homeostasis during injury via its intrinsic NMNAT activity.

Materials and methods

Reagents

FK866 ((E)-N-[4-(1-benzoylpiperidin-4-yl)butyl]-3-(pyridin-3-yl) acrylamide) was obtained from the National Institute of Mental Health Chemical Synthesis and Drug Supply Program (MH number F-901). Nimodipine was purchased from EMD Chemicals, Inc. (San Diego, CA). All other reagents were from Sigma-Aldrich (St. Louis, MO) unless otherwise noted.

Animals

All experimental procedures were conducted in accordance with the guidelines established by the National Academy of Sciences and overseen by the Animal Studies Committee at Washington University in St. Louis. Wild-type C57BL/6JOlaHsd (WT) and mutant C57BL/6JOlaHsd-Wld^S (Wld^S) mice were obtained from Harlan Laboratories (Blackthorn, UK). Animals of either sex were used in this study.

Compartmental culture and energy deprivation of cortical axons

Cortical axons were spatially separated from their somas and proximal neurites in culture using a two-compartment culture device as previously described (Shen and Goldberg, 2012). In brief, cortical neurons were dissociated from the cortices of either WT or Wld^S mice at embryonic day 15 (E15). The dissociated neurons were re-suspended in equal volumes of neuron culture medium containing 2% B27 and 0.5 mM glutamine in Neurobasal medium (Life Technologies, Grand Island, NY) and cultured upside-down as droplets for 5 h to reaggregate. The resulting cortical aggregates were cut into small pieces, 300–400 μm in size, and cultured in the neuron culture medium in the cell compartment of the two-compartment culture device. This culture device restrained the somas of cortical neurons in the cell compartment but allowed their axons to grow into the axon compartment. The fluid level in the cell compartment was set about 3 mm higher than that in the axon compartment. No equalization of fluid level between the two compartments was found for at least 48 h, indicating no significant fluid flow occurred between the two compartments. Every 3–4 days, half of the culture medium in both compartments was replaced with an axon culture medium containing 2% B27 and 0.5 mM Glutamax I in Neurobasal A medium (Life Technologies).

At 12–14 days in vitro (DIV), axons in the axon compartment were subjected to energy deprivation by being exposed to 6 mM sodium azide without glucose and pyruvate for 30 min in the presence or absence of the indicated drug treatments. These axons were then thoroughly washed before being further cultured in the axon culture medium for the indicated periods.

The structural integrity of axons was assessed by immunofluorescence staining with Tuj1 antibody (Covance, Emeryville, CA) as described in detail elsewhere (Shen and Goldberg, 2012). Consecutive epifluorescent images of the Tuj1-stained axons were taken from the proximal boundary of the cell and axon compartments to the axon terminals in the axon compartment. Montages were assembled with Adobe Photoshop CS2 (Adobe Systems Incorporated). The total number of intact axons in each montage was blindly quantified to the treatments at five arbitrary regions of interest (ROIs). The five ROIs were defined by five parallel lines spaced by 0.42 mm ranging 1.26 to 2.94 mm from the top of each montage. An intact axon was specified as one without beading or fragmentation.

Evaluation of ATP content

After 30 min of energy deprivation, both cell and axon compartments were washed with PBS. The cultures from either compartment were immediately lysed in 50 μl ice-cold lysis buffer containing 0.1 M Tris–HCl (pH 7.8), 1% Triton X-100, and 5 mM EDTA. ATP content from the above lysates was determined by luciferase and its substrate luciferin using an ATP determination kit (Life Technologies) according to the manufacturer's instructions and normalized by beta-actin contents in the corresponding lysates. Beta-actin content was determined by dot-blot using standard curves created from recombinant beta-actin (ProSci Incorporated, Poway, CA).

Determination of axon plasma membrane potential

The membrane potential of cortical axons was monitored with a voltage-sensitive fluorescent dye bis(1,3-dibutylbarbituric acid) trimethine oxonol ($Dibac_4(3)$; Life Technologies) as previously described (Shen and Goldberg, 2012). Briefly, axons were equilibrated with the dye (1 μM) in HCSS buffer containing 12 mM HEPES (pH 7.4), 1 mM NaH_2PO_4, 140 mM NaCl, 5 mM KCl, 0.8 mM $MgSO_4$, 1.8 mM $CaCl_2$, and 5.5 mM glucose at room temperature for 1 h. $Dibac_4(3)$ fluorescence was excited at 488 nm and collected via band-pass filter (505–530 nm) at 1 min intervals using a Zeiss LSM 5 PASCAL confocal microscope. For energy deprivation, after recording baseline $Dibac_4(3)$ fluorescence intensity (DFI) for 10 min (F0), the axon compartment was washed with glucose-free HCSS and then treated with 6 mM sodium azide in the same buffer in the presence of 1 μM $Dibac_4(3)$ for 30 min. At the end of the energy deprivation, all axons were thoroughly washed and then exposed to 50 mM potassium. The resulting potassium-depolarization response was used to confirm that all axons were loaded with $Dibac_4(3)$ and properly imaged. The average DFI of each culture (F) was determined from five to ten different axon fragments with ImageJ $1.38\times$ software (National Institutes of Health). The changes in plasma membrane potential are expressed as F/F0 ratio.

Determination of the changes in free calcium concentrations in cortical axons

Changes in free calcium concentration in axon ($[Ca^{2+}]_{axon}$) were monitored with Fura-2, a ratiometric calcium indicator. The indicator was loaded into cells by adding 5 μM Fura-2 acetoxymethyl (AM) ester (Invitrogen, Carlsbad, CA) and 0.1% Pluronic F-127 in HCSS to the cell compartment. After 60 min of incubation at room temperature, the indicator was washed off with HCSS. The culture was incubated for another 60 min for ester hydrolysis. Axons were then imaged on an inverted Nikon Eclipse microscope using a Neofluo $40\times/1.3$ oil

immersion objective and a cooled CCD camera (Cooke Corp., Auburn Hills, MI). Images were acquired at alternate excitation wavelengths (340/380 nm; 75 W xenon arc lamp) selected by band-pass filters (Semrock, Rochester, NY). The pairs of images were collected at 1 min intervals. After background subtraction, the matching images were divided by one another. The average ratio of each culture sample was determined in 20 to 30 ROIs randomly placed at different axons.

Energy deprivation was achieved by replacing HCSS in the axon compartment with glucose-free HCSS containing 6 mM sodium azide and 10 mM deoxyglucose for up to 40 min after acquiring six to ten baseline images. $[Ca^{2+}]_{axon}$ was calculated using the Grynkiewicz equation (Grynkiewicz et al., 1985):

$$\left[Ca^{2+}\right]_{axon} = K_d(R-R_f)/(R_b-R)(F_{2f}/F_{2b})$$

where K_d is the apparent dissociation constant, and R is the fluorescence intensity ratio. The symbols R_f and R_b are ratios of free and Ca^{2+}-bound indicators. F_{2f} and F_{2b} denote the second wavelength intensity of free and Ca^{2+}-bound indicators, respectively. The calibration constants were determined in calibration solutions.

Analysis of mitochondrial movement in axons

To label mitochondria, axons in the axon compartment were incubated with 200 nM MitoTracker Red CMXRos (MTR; Life Technologies) for 3 min. After washout of MTR, the culture was allowed to rest for 30 min at 37 °C and then placed in a customized flow chamber on the stage of an inverted microscope (Axiovert 200 M; Carl Zeiss Microimaging) equipped with a C-Apochromat 40×/1.2 water immersion lens and a Zeiss LSM 5 PASCAL confocal laser scanning module. The chamber was perfused with axon culture medium at a flow rate of 200 ml/h. The temperature in the flow chamber was maintained at 36.5 ± 0.5 °C with an inline heater (Warner Instruments, LLC, Hamden, CT). MTR fluorescence was excited with a 543 nm HeNe laser line and collected with a 560 nm long path filter. A series of 50 confocal images spaced 3 s apart were acquired at baseline, every 10 min during energy deprivation, and 10 min after energy deprivation. Kymographs were generated with an ImageJ Multiple Kymograph plugin written by J. Rietdorf (FMI Basel, Switzerland) and A. Seitz (EMBL Heidelberg, Germany). Fast mitochondrial movement was evaluated by counting the number of mitochondria with a moving velocity of at least 0.3 μm/s. The average number of total or fast-moving mitochondria was determined from approximately 10 different axon fragments in each sample, normalized by axon length, and shown as the number of total or fast-moving mitochondria per 100 μm of axon.

Assay of NMNAT enzymatic activity

NMNAT enzymatic activity was examined in cultured cortical neurons at 12 DIV. The neurons were lysed in an ice-cold lysis buffer containing 50 mM Tris–HCl (pH 7.4), 300 mM NaCl, 1 mM EDTA, 1% Triton X-100, and EDTA-free protease inhibitor cocktail (Roche Diagnostics GmbH, Mannheim, Germany) and then centrifuged at 10,000 ×g at 4 °C for 10 min. The total protein concentrations in the resulting supernatants were determined by a BCA Protein Assay Kit (Pierce Biotechnology, Rockford, IL), according to the manufacturer's instructions. NMNAT activity in the forward reaction (synthesis of NAD) was determined by a coupled enzymatic assay as previously described (Balducci et al., 1995; Schweiger et al., 2001; Yahata et al., 2009) with modifications. The assay was carried out in 100 μl reaction buffer containing 28 mM HEPES (pH 7.4), 16 mM Semicarbazide-HCl, 10 mM MgCl$_2$, 2 mM ATP, 6 units of alcohol dehydrogenase, and 30 μg of sample. The reactions were initiated by adding 2 mM NMN and performed at 37 °C for 1 h. The production of NADH (created from NAD by alcohol dehydrogenase) was measured by absorption at 340 nm with a Synergy

2 microplate reader (Biotek Instruments, Winooski, VT). One unit of NMNAT activity was defined as the amount of protein needed to produce 1 μmol of NAD per hour at 37 °C. To inhibit NMNAT activity, prior to the addition of NMN, the reaction buffer was preincubated with the indicated concentrations of gallotannin (GA) for 5 min at room temperature. The half maximal inhibitory concentration (IC_{50}) of GA was determined by fitting its dose-response data with the Four Parameter Logistic Equation using SigmaPlot 10.0 software (Systat Software, Inc., Chicago, IL).

Statistics

For each measurement, two or more experiments were independently performed at separate times using the same protocol. In each independent experiment, one or more independent cultures prepared from different mice were tested in each group. The sample size of each experimental group was determined by the number of independent cultures. The two-tailed *t*-test and the Mann–Whitney rank sum test were used to compare two groups for data with normal and non-normal distribution, respectively. The two-way analysis of variance (ANOVA) followed by the Tukey's post hoc test was used to compare many groups. The area under the curve (AUC) was determined by integrating the traces after baseline subtraction over a specified amount of time of indicated treatments. Statistical analyses were performed with SigmaStat 3.50 software (Systat Software, Inc). All data are expressed as mean ± SEM. Statistical significance was set at $P < 0.05$.

Results

Wld^S mutation alleviates the structural damage of CNS axons caused by energy deprivation

To evaluate the effects of Wld^S on axon injury caused by energy deprivation, we spatially separated cortical axons from their soma and proximal neurites using a two-compartment axon culture device (Shen and Goldberg, 2012); we then induced acute energy deprivation to axons by temporarily exposing the axons in the axon compartment with sodium azide (6 mM) in the absence of glucose and pyruvate for 30 min to inhibit both oxidative phosphorylation and glycolysis (Shen and Goldberg, 2012). After energy deprivation, the axons were thoroughly washed and further cultured in the original medium for up to 48 h. Because the loss of microtubule integrity is an early detectable event during axon degradation (Zhai et al., 2003), we used Tuj1 antibodies that recognize neuronal microtubules to compare the structural damage of WT and Wld^S axons at the indicated hours after energy deprivation. As shown in Fig. 1, transient energy deprivation led to widespread and progressive structural damage to WT axons. Axon beading throughout axon trajectories was detected as early as 4 h post injury (hpi). By 24 hpi axon beading was intensified; some axons became fragmented. At 48 hpi, a great majority of axons were severed or fully degenerated. In contrast, no obvious axon injury was found in Wld^S axons until 48 hpi, when axon beading was detected, whereas axon continuity was largely preserved. The percentages of intact axons in Wld^S cultures were significantly higher than those in WT cultures at all three time points investigated ($P < 0.05$). The data demonstrate that cortical axons are vulnerable to energy deprivation, and Wld^S reduces the resulting axon injury.

Wld^S mutation prevents axon ATP loss caused by energy deprivation

We then examined the ATP levels in WT and Wld^S cultures from either cell or axon compartment ($[ATP]_{cell}$ or $[ATP]_{axon}$) right after 30 min energy deprivation. In agreement with previous reports (Ikegami and Koike, 2003; Wang et al., 2005), $[ATP]_{cell}$ (Fig. 2A) and $[ATP]_{axon}$ (Fig. 2B) in untreated Wld^S culture were not different from those in WT culture; however, while energy deprivation
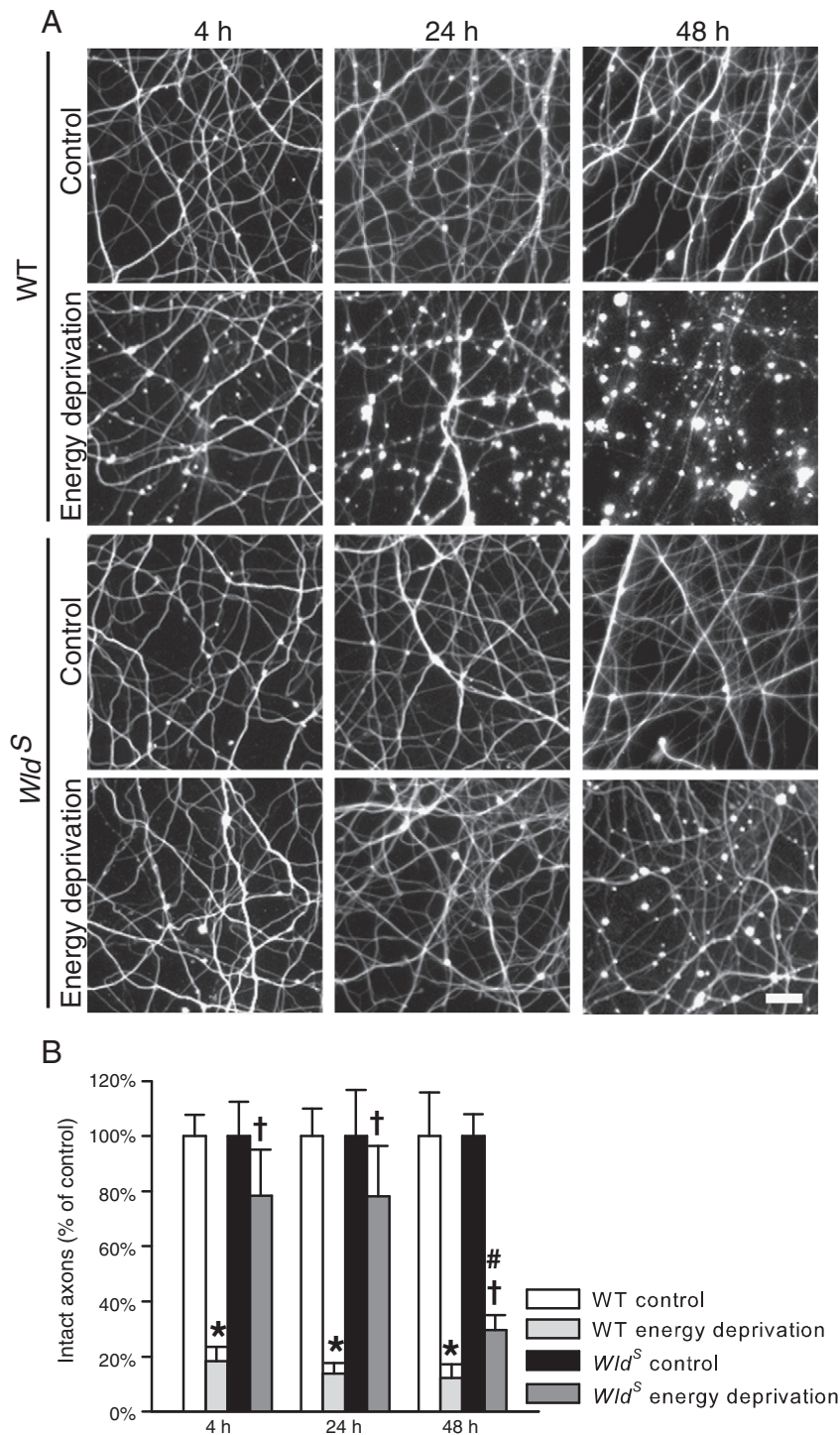
Fig. 1. Wld^S mutation alleviates axon damage caused by energy deprivation. A and B, Representative images (A) and quantification (B) of Tuj1-stained axons at the indicated hours after energy deprivation. The data are shown as a percentage of the respective control group. *, $P = <0.001$ compared to the corresponding WT control group; #, $P = <0.001$ compared to the corresponding Wld^S control group; †, $P < 0.05$ compared to the corresponding WT energy deprivation group. The data were collected from six to nine samples per group at each time point. Bar, 20 μm in A.

reduced WT $[ATP]_{axon}$ by over 65%, Wld^S $[ATP]_{axon}$ remained largely unchanged. Of note, energy deprivation in the axon compartment did not affect $[ATP]_{cell}$ in either WT or Wld^S culture (Fig. 2A), indicating this injury model is axon-selective.

To understand the temporal relationship between ATP loss and axon injury, we performed Tuj1 staining in both WT and Wld^S axons immediately after energy deprivation and did not detect any structural injury at this early time point (data not shown). Thus, axon ATP loss precedes

detectable axon degradation, and Wld^S is capable of preventing this early event.

Wld^S mutation reduces axon depolarization induced by energy deprivation

Most axon ATP is utilized by Na^+/K^+ pumps to maintain sodium and potassium gradients across plasma membrane that generate resting
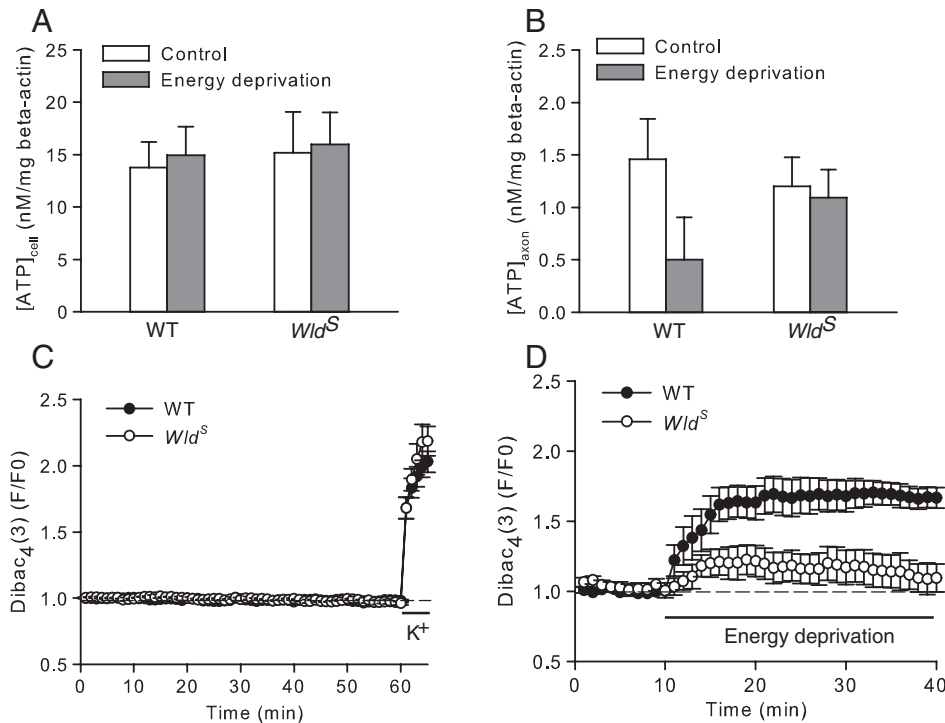
Fig. 2. Wld^S mutation retains ATP and plasma membrane potential in axons exposed to energy deprivation. A and B, ATP levels in the cell (A) and axon (B) compartment ($[ATP]_{cell}$ and $[ATP]_{axon}$) of either WT or Wld^S culture before (control) or right after 30 min energy deprivation (energy deprivation). The data were normalized by beta-actin contents in the respective samples. *, $P < 0.01$, compared to WT control group; †, $P < 0.05$ compared to WT energy deprivation group. The data were acquired from approximately 10 samples per group. C and D, Changes in $Dibac_4(3)$ fluorescence intensities (DFIs) in WT and Wld^S axons during rest and potassium depolarization (C) or energy deprivation (D). $Dibac_4(3)$ is a voltage-sensitive fluorescent dye. DFI rises in response to plasma membrane depolarization.

membrane potential (Ritchie, 1967). We and others have shown that energy deprivation impairs Na^+/K^+ pumps, depolarizes axons, disrupts intracellular ion homeostasis, and eventually leads to irreversible axon damage (Leppanen and Stys, 1997; Shen and Goldberg, 2012; Stys, 2005; Underhill and Goldberg, 2007). Since Wld^S prevented axon ATP loss caused by energy deprivation (Fig. 2B), we expected Wld^S axons to better maintain their membrane potential during energy deprivation and thereby block the downstream detrimental events.

To test this hypothesis, we compared the changes in membrane potential of WT and Wld^S axons during energy deprivation using a fluorescent membrane potential-sensitive dye $Dibac_4(3)$ (Braeuner et al., 1984). In untreated resting axons, $Dibac_4(3)$ fluorescence intensity (DFI) was stable for at least 60 min, but increased rapidly after potassium (50 mM) depolarization (Fig. 2C). Energy deprivation increased DFIs in both WT and Wld^S axons; however, the rate and the magnitude of the DFI rise in Wld^S axons were much smaller than those in WT axons (Fig. 2D), thus reporting a much suppressed depolarization response to energy deprivation. The average area under the DFI curves of Wld^S axons (4.66 ± 2.99, $n = 5$) during energy deprivation was significantly smaller than that of WT axons (18.37 ± 3.00, $n = 8$; $P = 0.011$, Wld^S vs. WT). The different depolarization response between the two types of axons is unlikely to reflect their differences in sodium/potassium channel properties, as the high potassium treatment resulted in virtually almost identical changes in WT and Wld^S membrane potentials (Fig. 2C). Therefore, it might be the well-maintained $[ATP]_{axon}$ in Wld^S axons that suppresses axon depolarization induced by energy deprivation.

Wld^S mutation partially suppresses the calcium influx into axoplasm caused by energy deprivation

Among the immediate consequences of plasma membrane depolarization is the opening of voltage-gated calcium channels (VGCCs) followed by massive free calcium accumulation in axoplasm; the latter may result in uncontrolled activation of many calcium-dependent processes that damage axons (Brown et al., 2001a,b; Fern et al., 1995; Schlaepfer and Bunge, 1973; Schlaepfer et al., 1985; Underhill and Goldberg, 2007). To see if this was the case in our energy deprivation model, we blocked calcium influx via L-type VGCC (L-VGCC) by applying nimodipine (10 μM) to the axon compartment during energy deprivation and examined axon structure by Tuj1 staining at 24 hpi. As shown in Fig. 3, the nimodipine treatment prevented WT axon damage caused by energy deprivation. No Wld^S axon damage was detected at this time point in the absence of nimodipine (Fig. 1), and the presence of nimodipine during energy depletion had no effect on Wld^S axon structure either (data not shown). Together, our data demonstrate that energy deprivation leads to activation of L-VGCC that results in calcium influx, and blocking this process prevents axon damage.

To further examine the process, we compared the changes in free calcium accumulation in WT and Wld^S axons during energy deprivation using the ratiometric calcium indicator Fura-2 (Grynkiewicz et al., 1985). Results showed that energy deprivation resulted in a slow but persistent increase in $[Ca^{2+}]_{axon}$ of both WT and Wld^S axons (filled circles in Figs. 4A and B; $n = 9$ and 6, respectively). Nevertheless, the average rate of free calcium accumulation in Wld^S axons (15–20 nM/min) was significantly lower ($P = 0.047$, compared by the slope) than that in WT axons (25–30 nM/min), resulting in lower $[Ca^{2+}]_{axon}$ in Wld^S than in WT axons ($P = 0.029$, two-way ANOVA). Most, if not all, of the calcium accumulation in the axoplasm occurred through the influx from the extra-axonal space, as removing calcium from buffer almost completely eliminated the Fura-2 signal changes (filled squares in Figs. 4A and B). Blocking L-VGCC with nimodipine during energy deprivation significantly reduced WT $[Ca^{2+}]_{axon}$ (open triangles in Fig. 4A; $n = 4$, $P < 0.001$, vs. energy depletion group), thus abolishing the above described differences in $[Ca^{2+}]_{axon}$ between WT and Wld^S axons
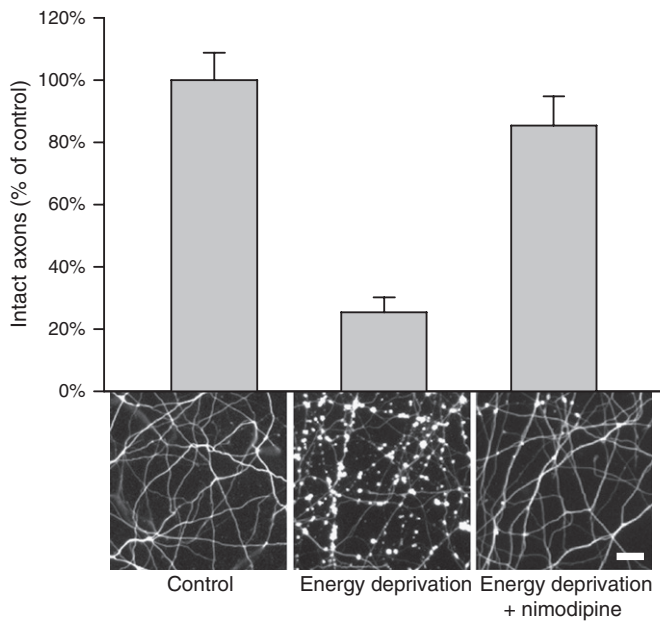
Fig. 3. Nimodipine protects axons against energy deprivation. The figure shows quantification and representative images of Tuj1-stained WT cortical axons at 24 h after the indicated treatments. The data were obtained from 10 samples per group. *, $P = <0.001$ compared to the other two groups. Bar, 20 μm.

As free calcium concentration measured with Fura-2 represents a balance between ion influx and efflux, the slower accumulation of free calcium in Wld^S axons during energy deprivation might result from the ability of Wld^S to curb the calcium influx, to promote calcium efflux, or to stimulate calcium uptake by mitochondria or other intracellular calcium stores. No matter which of these mechanisms plays a dominant role, our data indicate that the presence of Wld^S mutation reduces the harmful accumulation of free calcium in axoplasm, an effect that might contribute to the Wld^S-mediated axon protection (Fig. 1).

Intrinsic NMNAT activity is required for Wld^S to retain $[ATP]_{axon}$ during energy deprivation

Earlier studies have indicated that NMNAT activity is required for Wld^S to protect axons (Araki et al., 2004; Avery et al., 2009; Conforti et al., 2009; Yahata et al., 2009). We wondered if NMNAT is also necessary for Wld^S to maintain energy homeostasis in axons. Moreover, because Wld^S $[ATP]_{axon}$ was higher than WT $[ATP]_{axon}$ during energy deprivation but not under normal conditions (Fig. 2B), we also wanted to know if the NMNAT activity provided by Wld^S is only required during metabolic stress.

To answer these questions, we first compared NMNAT activity in the cultured cortical neurons from Wld^S and WT mice using a photometric assay (Balducci et al., 1995; Schweiger et al., 2001; Yahata et al., 2009). The result showed that NMNAT activity in Wld^S neurons was significantly higher than that in WT neurons under normal conditions (Fig. 5A; $P < 0.05$). Next, we chose GA, a putative NMNAT inhibitor (Berger et al., 2005), to temporarily reduce NMNAT activity during energy deprivation. As expected, GA dose-dependently reduced NMNAT activity in both WT and Wld^S neurons, but it did not eliminate their difference in enzymatic activity (Fig. 5A; $P < 0.05$). The calculated IC_{50} of GA for NMNAT activity in WT and Wld^S neurons was 3.7 μM and 3.8 μM, respectively, similar to that reported by Berger et al. (2005). Therefore, we used 4 μM GA in the subsequent experiments to partially inhibit WT and Wld^S NMNAT activity. GA is toxic to cortical neurons at concentrations above 10 μM (data not shown). The inhibitor was added to the axon compartment either just before energy deprivation for 40 min and then washed out (pretreatment), or from 10 min before
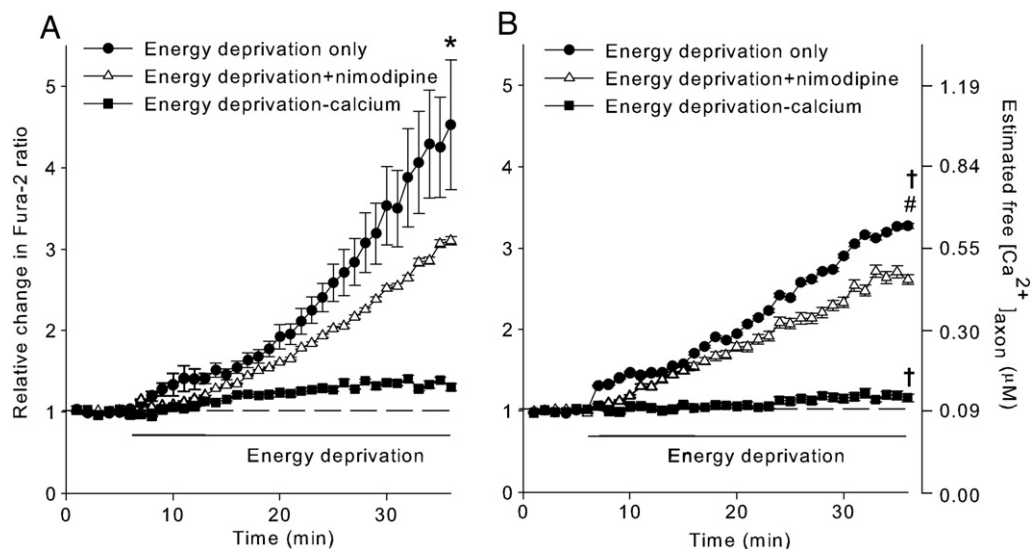
(comparing the open triangles in Figs. 4A and B, $P = 0.823$). In contrast, nimodipine was less effective in blocking calcium from entering Wld^S axons, as only a small reduction in $[Ca^{2+}]_{axon}$ was detected in nimodipine-treated Wld^S axons (open triangles in Fig. 4B, n = 4). Together, the results suggest that L-VGCC is an important route of calcium influx in WT axons during energy deprivation. As nimodipine failed to completely prevent calcium accumulation, in addition to L-VGCC, calcium likely enters axons via other nimodipine-insensitive VGCC and/or Na^+/Ca^{2+} exchanger operated in the reverse mode as well.

Fig. 4. Wld^S mutation suppresses free calcium accumulation in axons during energy deprivation. A and B, Changes of free calcium levels in axoplasm ($[Ca^{2+}]_{axon}$) of WT (A) and Wld^S (B) axons during energy deprivation. Using Fura-2, a ratiometric calcium indicator, $[Ca^{2+}]_{axon}$ was determined by measuring the relative change of Fura-2 ratio in axons treated with energy deprivation only, energy deprivation plus 10 μM nimodipine (energy deprivation + nimodipine), and energy deprivation in calcium-free buffer supplemented with 20 μM EGTA (energy deprivation − calcium), respectively. Statistical analysis was performed with two-way ANOVA. *, $P = <0.001$ compared to any other WT group; #, $P = <0.001$ compared to any other Wld^S group; †, $P < 0.05$ compared to the corresponding WT group.
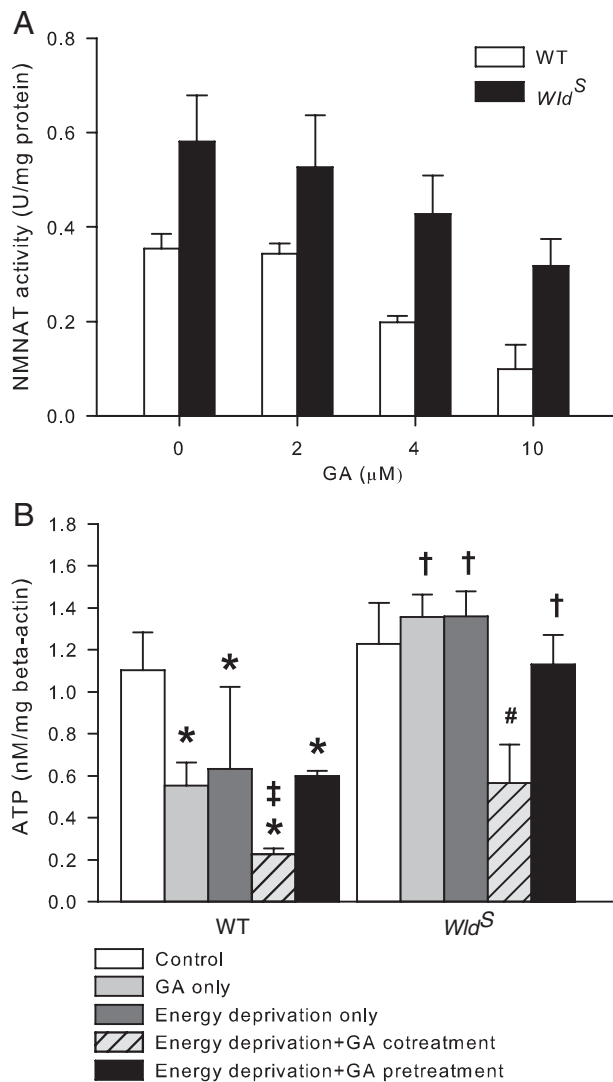
Fig. 5. Intrinsic NMNAT activity is required for *Wld^S* to retain energy homeostasis in axons during but not prior to energy deprivation. A, Dose effect of GA on NMNAT activity. NMNAT activity in cultured cortical neurons at 12 DIV was determined in the presence and absence of the indicated doses of GA. N = 3 to 5 per group. B, Effect of NMNAT inhibition on axon ATP levels. The ATP level in axons was assessed after the following treatments: sham wash and vehicle control (control), 40 min GA (GA only), 30 min energy deprivation (energy deprivation only), 10 min GA pretreatment followed by 30 min energy deprivation with GA (energy deprivation + GA cotreatment), and 40 min GA followed by thorough wash and 30 min energy deprivation without GA (energy deprivation + GA pretreatment). The data were acquired from approximately seven samples per group. *, $P < 0.05$ compared to WT control group; ‡, $P < 0.05$ compared to WT GA only and WT energy deprivation + GA pretreatment groups; #, $P < 0.05$ compared to all other *Wld^S* groups; †, $P < 0.05$ compared to the corresponding WT group.

the onset until the end of energy deprivation (cotreatment). Axon ATP levels were then determined at the end of energy deprivation. Under control conditions, GA reduced WT $[ATP]_{axon}$ by 50% but had no effect on *Wld^S* $[ATP]_{axon}$ (Fig. 5B). When GA was present during energy deprivation, it markedly reduced $[ATP]_{axon}$ in both WT and *Wld^S* cultures by 80% and 54%, respectively. In contrast, GA pretreatment did not affect $[ATP]_{axon}$ in either WT or *Wld^S* axons subjected to energy deprivation (Fig. 5B; $P > 0.05$, energy depletion + GA pretreatment vs. energy deprivation only). Thus, while WT NMNAT activity is critical for maintaining $[ATP]_{axon}$ under both normal and energy deprived conditions; the higher than normal NMNAT activity provided by *Wld^S* is only required to retain $[ATP]_{axon}$ during energy deprivation.

Intrinsic NMNAT activity is required for *Wld^S* to protect axons against energy deprivation

If the higher than normal NMNAT activity and the subsequent ATP preservation during energy deprivation are essential for *Wld^S* to protect axons, inhibition of *Wld^S* NMNAT activity during the period would be sufficient to abolish the axon protection. To test this hypothesis, we examined axon injury at 24 h after the treatments described in Fig. 5B. In accord with its effects on NMNAT activity (Fig. 5A) and $[ATP]_{axon}$ (Fig. 5B), GA treatment alone was sufficient to injure WT but not *Wld^S* axons (Fig. 6); limiting NMNAT activity before energy deprivation neither affected *Wld^S* axons nor aggravated WT axon injury caused by energy deprivation; in contrast, reducing NMNAT activity during energy deprivation not only exaggerated WT axon injury but also injured *Wld^S* axons. There was a good correlation between $[ATP]_{axon}$ (Fig. 5B) and structural integrity (Fig. 6B) for both WT ($R^2 = 0.938$, $P = 0.0182$, Pearson Product Moment Correlation) and *Wld^S* axons ($R^2 = 0.954$, $P = 0.0118$, Pearson Product Moment Correlation). Together, these data demonstrate that the intrinsic *Wld^S* NMNAT activity is necessary for the mutation to both retain axon ATP during energy deprivation and reduce the subsequent structural damage. These data also strongly support the idea that maintaining axon energy homeostasis is essential for *Wld^S*-mediated axon protection.

Inhibiting NMNAT-catalyzed NAD synthesis increases $[ATP]_{axon}$ and protects axons from energy deprivation

To test if the production of NAD by NMNAT is necessary for the *Wld^S*-mediated axon energy homeostasis and protection, we used FK866 to inhibit the process. FK866 is a highly specific, tight-binding nicotinamide phosphoribosyltransferase (NAMPT) inhibitor (Hasmann and Schemainda, 2003; Khan et al., 2006). As illustrated in Fig. 7A, NAMPT, together with NMNAT, constitutes the salvage pathway of NAD resynthesis from nicotinamide (NAM; Lau et al., 2009). By blocking the first step of the pathway, FK866 reduces the availability of NMN (Formentini et al., 2009; Hasmann and Schemainda, 2003) and the subsequent biosynthesis of NAD by NMNAT (Hasmann and Schemainda, 2003; Pittelli et al., 2010; Sasaki et al., 2009). FK866 neither directly reduces cellular ATP level (Hasmann and Schemainda, 2003; Pittelli et al., 2010) nor affects mitochondrial ATP production (Pittelli et al., 2010) and NMNAT activity (Berger et al., 2005; Formentini et al., 2009). The inhibitor (1 μM) was applied to the axon compartment for 1 h. This dosage was chosen based on previous report (Pittelli et al., 2010) and our pilot study, which reduced NAD contents in cultured cortical neurons by about 15%. After the treatment, axons were subjected to energy deprivation and then lysed for ATP measurement. As shown in Fig. 7B, under control conditions, this FK866 treatment led to a tendency of increase rather than decrease in both WT and *Wld^S* $[ATP]_{axon}$ by 21% and 16%, respectively. This result is consistent with those reported by Pittelli et al. (2010). Most interestingly, when the treatment was followed by energy deprivation, it significantly increased WT $[ATP]_{axon}$ by over 50% ($P < 0.05$, WT energy deprivation only vs. WT FK866 + energy deprivation), and the same treatment caused a much larger, 3.8-fold increase in *Wld^S* $[ATP]_{axon}$ (Fig. 7B). Thus, in line with previous report (Sasaki et al., 2009), despite the requirement for NMNAT activity in axon energy homeostasis during energy deprivation, the NMNAT-catalyzed NAD synthesis is not necessary for the effect. In contrast, inhibition of this reaction improves axon bioenergetics.

To further elucidate the causal relationship between $[ATP]_{axon}$ and structural integrity, we examined the effect of FK866 on axon structure at 24 h after energy deprivation. We found that, the FK866 pretreatment, which limited ATP reduction in WT axons (Fig. 7B), considerably reduced axon damage caused by energy deprivation (Fig. 8). As expected, FK866 did not affect the structure of *Wld^S* axons when applied alone or in combination with energy deprivation (Fig. 8). Taken together, the results
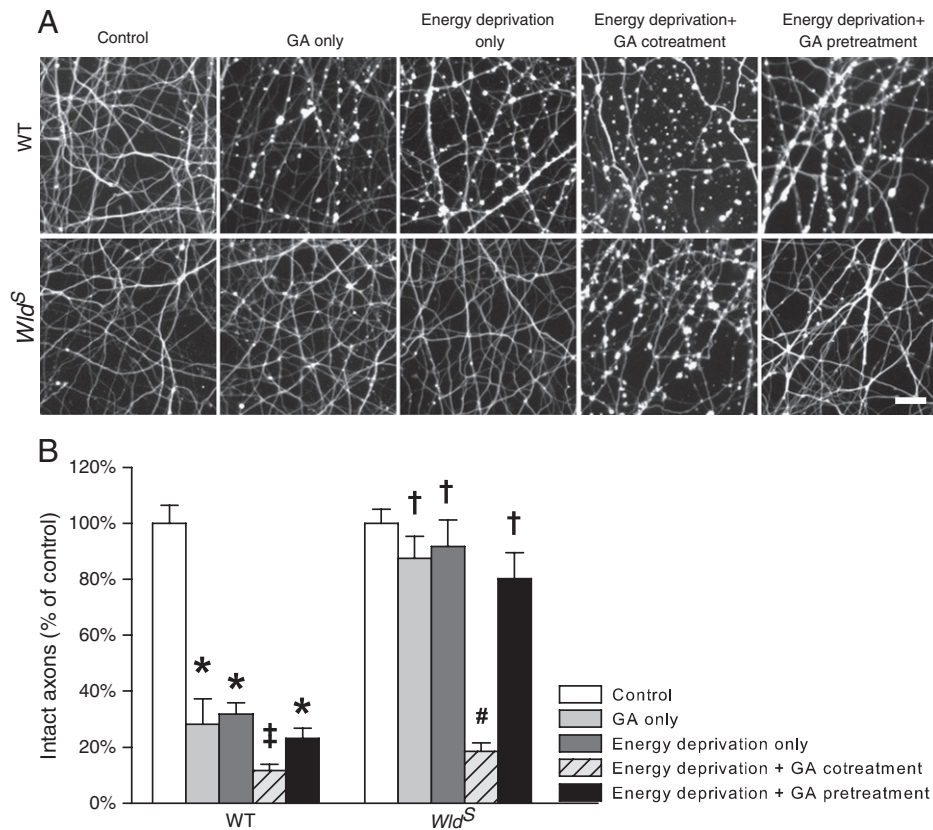
Fig. 6. Intrinsic NMNAT activity is required for Wld^S to protect axons from energy deprivation. A and B, Representative images (A) and quantification (B) of Tuj1-stained cortical axons at 24 h after the indicated treatments. The data were acquired from an average of seven samples per group. *, $P = <0.001$ compared to WT control; ‡, $P < 0.05$ compared to all other WT groups; #, $P = <0.001$ compared to all other Wld^S groups; †, $P = <0.001$ compared to the corresponding WT group. Bar, 20 μm in A.

indicate that improving $[ATP]_{axon}$ but not promoting NAD synthesis is essential for Wld^S NMNAT to protect axons against energy deprivation.

Discussion

Wld^S mutation encodes a chimeric protein (Coleman et al., 1998; Mack et al., 2001) that has been found to delay or attenuate axon degeneration in experimental models of many neurological disorders

(Adalbert et al., 2006; Ferri et al., 2003; Gillingwater et al., 2004, 2006; Hasbani and O'Malley, 2006; Kaneko et al., 2006; Ryu et al., 2006; Sajadi et al., 2004). Although many mechanisms of Wld^S-mediated axon protection have been suggested (Araki et al., 2004; Avery et al., 2012; Conforti et al., 2009; Gilley and Coleman, 2010; Press and Milbrandt, 2008; Wang et al., 2005; Yahata et al., 2009), the issue remains obscure. We examined the possibility that Wld^S exerts its protective effects by preventing energy loss commonly occurring in a number of
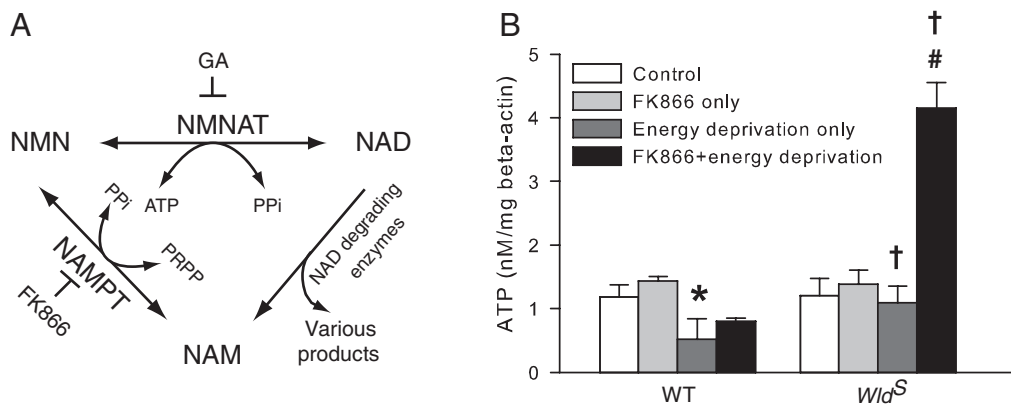

Fig. 7. Inhibiting NMNAT-catalyzed NAD synthesis by FK866 alleviates axon ATP loss caused by energy deprivation. A, Schematic illustration of the salvage pathway of NAD resynthesis from NAM. The salvage pathway utilizes NAM produced by such constitutive NAD degrading enzymes as poly(ADP-ribose) polymerases, ADP-ribose transferasses, cADP-ribose synthases, and sirtuins to resynthesize NAD at the expense of ATP. The pathway consists of two consecutive reactions catalyzed by NAMPT and NMNAT, respectively. FK866 specifically blocks the production of NMN by NAMPT. GA is a putative inhibitor of NMNAT. B, FK866 reduces axon ATP loss caused by energy deprivation. WT and Wld^S $[ATP]_{axon}$ were determined immediately after the following treatments: sham wash and vehicle control (control), FK866 for 1 h (FK866 only), energy deprivation for 30 min (energy deprivation only), and FK866 for 1 h followed by 30 min energy deprivation in the absence of FK866 (FK866 + energy deprivation). The data were acquired from an average of eight samples per group. *, $P < 0.05$ compared to any other WT group; #, $P = <0.001$ compared to any other Wld^S group; †, $P < 0.05$ compared to the corresponding WT group.
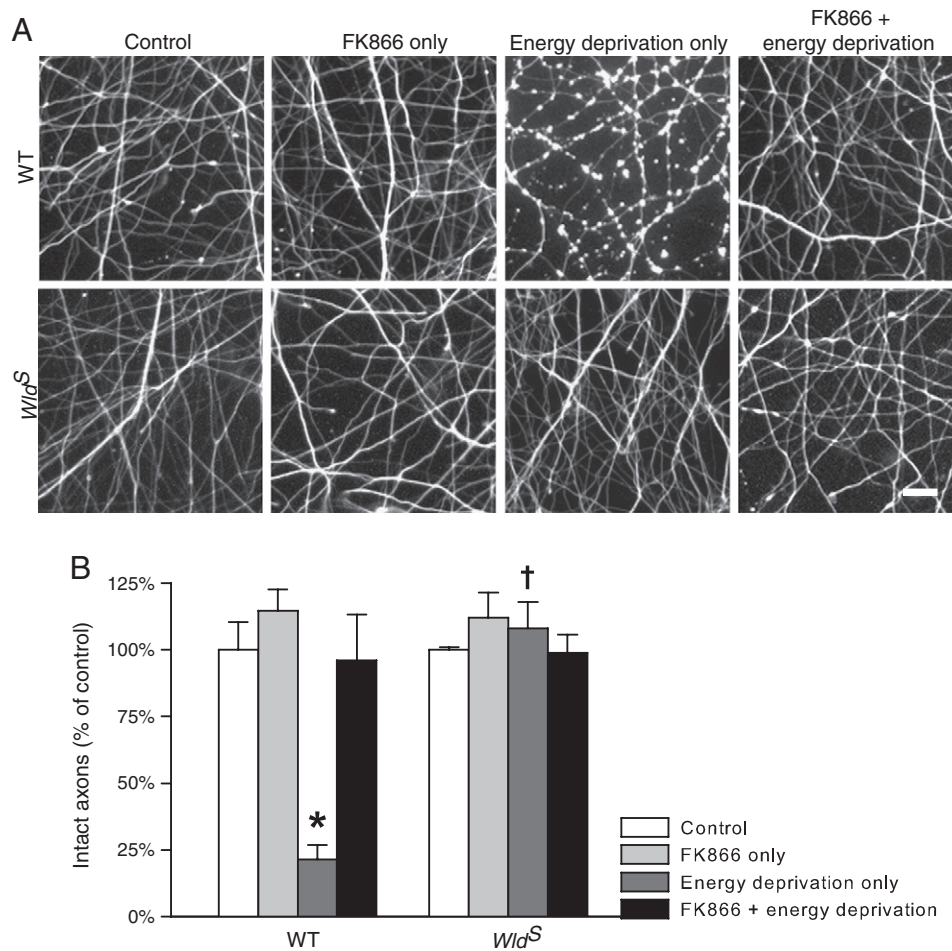
Fig. 8. Improving axon energy homeostasis with FK866 protects axons against energy deprivation. A and B, Representative images (A) and quantification (B) of Tuj1-stained cortical axons from WT and *Wld^S* cultures at 24 h after the treatments as described in Fig. 7B. The data were obtained from an average of seven samples per group. *, $P = <0.001$ compared to any other WT group; †, $P = <0.001$ compared to the corresponding WT group. Bar, 20 μm in A.

neurological disorders (Goldberg and Ransom, 2003; Mattson and Liu, 2002; Stys, 2004, 2005; Trapp and Stys, 2009; Waxman, 2006). Using a compartmental axon culture model (Shen and Goldberg, 2012), we analyzed the relationship between axon injury and ATP level after acute energy deprivation. Deprivation of metabolic substrates results in axon degeneration, and *Wld^S* mutation inhibits events leading from energy deficiency to axon degeneration. Furthermore, our results demonstrate a close link between the abilities of *Wld^S* to improve axon energy homeostasis and to reduce structural damage. Taken together, these data suggest that enhanced energy maintenance might be essential for *Wld^S* to protect axons from degeneration.

Energy deficiency, axon injury, and Wld^S-mediated axon protection

Using the energy deprivation model, this study has shown that energy deficiency leads to axon injury, while improving axon energy homeostasis either by *Wld^S* mutation or pharmacologically creating conditions favoring ATP over NAD synthesis by NMNAT protects axons. This observation is consistent with that of previous reports that have implicated energy loss in axon degeneration and its prevention by *Wld^S* mutation. In particular, energy restriction has been suggested as the primary cause of Wallerian degeneration in an in vivo study (Alvarez et al., 2008), while *Wld^S* has been reported to maintain cellular ATP levels and protect axons against other insults such as vinblastine toxin and axotomy (Ikegami and Koike, 2003; Wang et al., 2005). Furthermore, a recent study has revealed a

higher capacity of mitochondrial ATP production in *Wld^S* and NMNAT3 (mitochondrial isoform of NMNAT) transgenic mice (Yahata et al., 2009). On the other hand, it has also been reported that substantial reduction of neuronal ATP level by glycolysis inhibition was not sufficient to damage axons, and increasing neuronal ATP level by tetrodotoxin (TTX) failed to protect axons from rotenone toxin (Press and Milbrandt, 2008). This discrepancy is yet to be reconciled. It might be in part due to the differences in injury models and in part due to the complexity of maintaining ATP homeostasis in axons and their cell bodies (Tolkovsky and Suidan, 1987).

Wld^S-mediated energy homeostasis and NMNAT activity

We have showed that *Wld^S* prevents axon ATP loss after energy deprivation (Fig. 2B), an effect dependent on its intrinsic NMNAT activity during but not prior to energy deprivation (Fig. 5B). Because NMNAT is a NAD-synthesizing enzyme, and NAD, as a coenzyme, plays an important role in energy metabolism by accepting and providing electrons, it has been proposed that excess NMNAT activity in *Wld^S* might prevent ATP decrease by maintaining local NAD level (Wang et al., 2005). However, this process demands metabolic substrates and healthy mitochondria, which are often compromised during axon injury (Coleman, 2005; Mattson and Liu, 2002; Stys, 2005; Waxman, 2006). There is convincing evidence demonstrating that NMNAT-mediated axon protection is independent of NAD level (Sasaki et al., 2009). Moreover, if ATP homeostasis is critical for *Wld^S*-mediated axon protection, then enhanced

synthesis of NAD via forward operation of NMNAT might be harmful, as the reaction consumes ATP (Berger et al., 2005; Pittelli et al., 2010). Here we show that inhibiting NMNAT-catalyzed NAD synthesis by limiting the availability of the reaction substrate NMN did, in fact, reduce $[ATP]_{axon}$ loss (Fig. 7B) and axon injury (Fig. 8) caused by energy deprivation. Thus, NAD is unlikely to be the enzymatic product of NMNAT that is responsible for Wld^S-mediated energy homeostasis.

Interestingly, although NMNAT is generally considered to be an NAD-synthesizing enzyme under physiological conditions (Lau et al., 2009), the enzyme was originally identified as a NAD-pyrophosphorylase (Kornberg and Lindberg, 1948), and its kinetic constants favor the reverse reaction (Berger et al., 2005). It is possible that a change in substrate availability (e.g., a shortage of either ATP or NMN, or both), might drive NMNAT into its reverse mode that directly produces ATP (Fig. 7A). This idea may explain why FK866, which blocks the synthesis of the NAD precursor NMN, essentially increased ATP levels in axons subjected to energy deprivation (Fig. 7B). It may also explain why Wld^S increased $[ATP]_{axon}$ only when their axons were exposed to energy deprivation (Fig. 2B), and why excess NMNAT activity was only required for Wld^S protection during this particular period (Figs. 5B and 6). The different efficiencies of FK866 in increasing ATP levels in WT and Wld^S axons after energy deprivation may reflect different NMNAT activities in these two types of axons and therefore different abilities to create ATP. On the other hand, excess NAD may favor reverse operation of NMNAT as well. Consistently, it has been demonstrated that exogenous NAD leads to a dose-dependent increase in $[ATP]_{axon}$ after axotomy, and this increase is correlated with greater axon protection (Wang et al., 2005).

To maintain ATP synthesis via its reverse reaction, NMNAT would require a supply of the NAD substrate (Fig. 7A), which has been found to accumulate in the mitochondria (Yager et al., 1991; Yang et al., 2007) and multiple tissues (Chen et al., 2008) of rodents deprived of metabolic substrates. Besides NAD, NMNAT may utilize other dinucleotides, such as NADH and nicotinic acid adenine dinucleotide, to produce ATP as well (Berger et al., 2005). On the other hand, energy deficiency would be a prerequisite to initiate the reverse operation of NMNAT. Even though the overall Wld^S $[ATP]_{axon}$ was largely normal (Fig. 2B), a transient energy deficiency might have occurred in Wld^S axons at the onset of energy deprivation, thus resulting in partial axon depolarization. To further examine the possibility, it would be necessary to perform dynamic analysis of axon ATP, NAD, and NMN levels during and immediately after energy deprivation in the presence and absence of FK866 treatment, and to test if one may interfere with the Wld^S/NMNAT-mediated axon protection by manipulating the levels of these metabolites in axons and therefore the direction of NMNAT-catalyzed reaction during energy deprivation.

Because mitochondria are not only the primary sites of ATP production but also the potential key sites of Wld^S action (Avery et al., 2012; Fang et al., 2012; Yahata et al., 2009), we cannot rule out the possibility that Wld^S/NMNAT may augment mitochondrial function, biogenesis, or axonal transport and therefore facilitate local energy homeostasis during axon injury. The previously published data seem to speak against this idea. In particular, no changes in protein expression and enzymatic activity of any respiratory complex have been detected in mitochondria from either NMNAT 3 transgenic or Wld^S mice (Yahata et al., 2009). Besides, Wld^S has no direct impact on mitochondrial permeability transition pore formation (Barrientos et al., 2011). To test this notion further, we compared the mitochondrial density, distribution, and mobility in WT and Wld^S cortical axons. Results showed no obvious differences between the two types of axons under normal conditions (Supplemental Figs. 1A and 1B, 0 min, and data not shown). Energy deprivation almost completely blocked the bidirectional fast movement of WT mitochondria (Supplemental Fig. 1B) without changing their density and distribution (Supplemental Fig. 1A and data not shown). This effect was only partially reversed during recovery (Supplemental Fig. 1B). The presence of Wld^S mutation resulted in significant improvement in mitochondrial mobility during energy

deprivation and recovery (Supplemental Fig. 1B, $P < 0.001$, two-way ANOVA). Nevertheless, this protective effect of Wld^S is most likely due to its ability to control $[Ca^{2+}]_{axon}$ (Fig. 4B), as mitochondrial mobility is regulated by free calcium level (Avery et al., 2012; Wang and Schwarz, 2009; Yi et al., 2004). This idea is supported by our observation that, nimodipine, which reduced calcium influx during energy deprivation (Fig. 4A), also effectively improved mitochondrial movement in WT axons (data not shown). In addition, as mitochondrial movement is an energy-consuming process, and mitochondrial mobility has been suggested to be regulated by ATP demand (Hollenbeck, 1996; Saxton and Hollenbeck, 2012), the improved axon energy status provided by Wld^S may further facilitate mitochondrial movement during energy deprivation.

Wld^S-mediated axon protection and axon degeneration

The fact that Wld^S mutation protects axons in a wide variety of models of neurological disorders suggests that the mutation might control a single common factor that determines the survival or degeneration fate of axons. The nature of this factor currently is a subject of a heated discussion. Here we have shown that Wld^S improves axon energy homeostasis during energy deprivation possibly through reverse activation of NMNAT activity to generate ATP. In doing so, Wld^S provides much needed energy for different processes essential for axon function and survival, including supporting Na^+/K^+ pump to maintain ion gradients and membrane potential, preventing adverse calcium influx via VGCC, facilitating plasma membrane calcium ATPase to exclude excessive free calcium, and sustaining mitochondrial movement. These effects in turn may further facilitate axon energy homeostasis. Thus, energy failure might be the common factor that leads to the final program of axon degeneration, and ATP might be the axon survival factor provided by Wld^S via NMNAT.

Taken together, our findings suggest a new mechanism for Wld^S-mediated axon protection. Experimental approaches to increasing NMNAT activity during injury or to sustaining axon bioenergetics (e.g. by FK866), may be protective in axon injuries associated with energy deficiency.

Supplementary data to this article can be found online at http://dx.doi.org/10.1016/j.nbd.2013.07.007.

References

Adalbert, R., Nógrádi, A., Szabó, A., Coleman, M.P., 2006. The slow Wallerian degeneration gene in vivo protects motor axons but not their cell bodies after avulsion and neonatal axotomy. Eur. J. Neurosci. 24, 2163–2168.
Alvarez, S., Moldovan, M., Krarup, C., 2008. Acute energy restriction triggers Wallerian degeneration in mouse. Exp. Neurol. 212, 166–178.
Araki, T., Sasaki, Y., Milbrandt, J., 2004. Increased nuclear NAD biosynthesis and SIRT1 activation prevent axonal degeneration. Science 305, 1010–1013.
Avery, M.A., Sheehan, A.E., Kerr, K.S., Wang, J., Freeman, M.R., 2009. Wld^S requires Nmnat1 enzymatic activity and N16-VCP interactions to suppress Wallerian degeneration. J. Cell Biol. 184, 501–513.
Avery, M.A., Rooney, T.M., Pandya, J.D., Wishart, T.M., Gillingwater, T.H., Geddes, J.W., et al., 2012. Wld(s) prevents axon degeneration through increased mitochondrial flux and enhanced mitochondrial ca(2+) buffering. Curr. Biol. 22, 596–600.

Balducci, E., Emanuelli, M., Raffaelli, N., Ruggieri, S., Amici, A., Magni, G., et al., 1995. Assay methods for nicotinamide mononucleotide adenylyltransferase of wide applicability. Anal. Biochem. 228, 64–68.

Barrientos, S.A., Martinez, N.W., Yoo, S., Jara, J.S., Zamorano, S., Hetz, C., et al., 2011. Axonal degeneration is mediated by the mitochondrial permeability transition pore. J. Neurosci. 31, 966–978.

Berger, F., Lau, C., Dahlmann, M., Ziegler, M., 2005. Subcellular compartmentation and differential catalytic properties of the three human nicotinamide mononucleotide adenylyltransferase isoforms. J. Biol. Chem. 280, 36334–36341.

Braeuner, T., Huelser, D.F., Strasser, R.J., 1984. Comparative measurements of membrane potentials with microelectrodes and voltage-sensitive dyes. Biochim. Biophys. Acta 771, 208–216.

Brown, A.M., Wender, R., Ransom, B.R., 2001a. Ionic mechanisms of aglycemic axon injury in mammalian central white matter. J. Cereb. Blood Flow Metab. 21, 385–395.

Brown, A.M., Westenbroek, R.E., Catterall, W.A., Ransom, B.R., 2001b. Axonal L-type Ca^{2+} channels and anoxic injury in rat CNS white matter. J. Neurophysiol. 85, 900–911.

Chen, D., Bruno, J., Easlon, E., Lin, S.J., Cheng, H.L., Alt, F.W., et al., 2008. Tissue-specific regulation of SIRT1 by calorie restriction. Genes Dev. 22, 1753–1757.

Coleman, M., 2005. Axon degeneration mechanisms: commonality amid diversity. Nat. Rev. Neurosci. 6, 889–898.

Coleman, M.P., Conforti, L., Buckmaster, E.A., Tarlton, A., Ewing, R.M., Brown, M.C., et al., 1998. An 85-kb tandem triplication in the slow Wallerian degeneration (Wlds) mouse. Proc. Natl. Acad. Sci. U. S. A. 95, 9985–9990.

Conforti, L., Wilbrey, A., Morreale, G., Janeckova, L., Beirowski, B., Adalbert, R., et al., 2009. WldS protein requires Nmnat activity and a short N-terminal sequence to protect axons in mice. J. Cell Biol. 184, 491–500.

Fang, Y., Soares, L., Teng, X., Geary, M., Bonini, N.M., 2012. A novel Drosophila model of nerve injury reveals an essential role of Nmnat in maintaining axonal integrity. Curr. Biol. 22, 590–595.

Fern, R., Ransom, B.R., Waxman, S.G., 1995. Voltage-gated calcium channels in CNS white matter: role in anoxic injury. J. Neurophysiol. 74, 369–377.

Ferri, A., Sanes, J.R., Coleman, M.P., Cunningham, J.M., Kato, A.C., 2003. Inhibiting axon degeneration and synapse loss attenuates apoptosis and disease progression in a mouse model of motoneuron disease. Curr. Biol. 13, 669–673.

Formentini, L., Moroni, F., Chiarugi, A., 2009. Detection and pharmacological modulation of nicotinamide mononucleotide (NMN) in vitro and in vivo. Biochem. Pharmacol. 77, 1612–1620.

Gilley, J., Coleman, M.P., 2010. Endogenous Nmnat2 is an essential survival factor for maintenance of healthy axons. PLoS Biol. 26, e1000300.

Gillingwater, T.H., Haley, J.E., Ribchester, R.R., Horsburgh, K., 2004. Neuroprotection after transient global cerebral ischemia in Wld(s) mutant mice. J. Cereb. Blood Flow Metab. 24, 62–66.

Gillingwater, T.H., Ingham, C.A., Parry, K.E., Wright, A.K., Haley, J.E., Wishart, T.M., et al., 2006. Delayed synaptic degeneration in the CNS of Wlds mice after cortical lesion. Brain 129, 1546–1556.

Goldberg, M.P., Ransom, B.R., 2003. New light on white matter. Stroke 34, 330–332.

Grynkiewicz, G., Poenie, M., Tsien, R.Y., 1985. A new generation of Ca^{2+} indicators with greatly improved fluorescence properties. J. Biol. Chem. 260, 3440–3450.

Hasbani, D.M., O'Malley, K.L., 2006. Wld(S) mice are protected against the Parkinsonian mimetic MPTP. Exp. Neurol. 202, 93–99.

Hasmann, M., Schemainda, I., 2003. FK866, a highly specific noncompetitive inhibitor of nicotinamide phosphoribosyltransferase, represents a novel mechanism for induction of tumor cell apoptosis. Cancer Res. 63, 7436–7442.

Hollenbeck, P.J., 1996. The pattern and mechanism of mitochondrial transport in axons. Front. Biosci. 1, 91–102.

Ikegami, K., Koike, T., 2003. Non-apoptotic neurite degeneration in apoptotic neuronal death: pivotal role of mitochondrial function in neurites. Neuroscience 122, 617–626.

Kaneko, S., Wang, J., Kaneko, M., Yiu, G., Hurrell, J.M., Chitnis, T., et al., 2006. Protecting axonal degeneration by increasing nicotinamide adenine dinucleotide levels in experimental autoimmune encephalomyelitis models. J. Neurosci. 26, 9794–9804.

Khan, J.A., Tao, X., Tong, L., 2006. Molecular basis for the inhibition of human NMPRTase, a novel target for anticancer agents. Nat. Struct. Mol. Biol. 13, 582–588.

Kornberg, A., Lindberg, O., 1948. Diphosphopyridine nucleotide pyrophosphatase. J. Biol. Chem. 176, 665–677.

Lau, C., Niere, M., Ziegler, M., 2009. The NMN/NaMN adenylyltransferase (NMNAT) protein family. Front. Biosci. 14, 410–431.

Leppanen, L., Stys, P.K., 1997. Ion transport and membrane potential in CNS myelinated axons. II. Effects of metabolic inhibition. J. Neurophysiol. 78, 2095–2107.

Lunn, E.R., Perry, V.H., Brown, M.C., Rosen, H., Gordon, S., 1989. Absence of Wallerian degeneration does not hinder regeneration in peripheral nerve. Eur. J. Neurosci. 1, 27–33.

Mack, T.G., Reiner, M., Beirowski, B., Mi, W., Emanuelli, M., Wagner, D., et al., 2001. Wallerian degeneration of injured axons and synapses is delayed by a Ube4b/Nmnat chimeric gene. Nat. Neurosci. 4, 1199–1206.

Mattson, M.P., Liu, D., 2002. Energetics and oxidative stress in synaptic plasticity and neurodegenerative disorders. Neuromolecular Med. 2, 215–231.

Pittelli, M., Formentini, L., Faraco, G., Lapucci, A., Rapizzi, E., Cialdai, F., et al., 2010. Inhibition of nicotinamide phosphoribosyltransferase: cellular bioenergetics reveals a mitochondrial insensitive NAD pool. J. Biol. Chem. 285, 34106–34114.

Press, C., Milbrandt, J., 2008. Nmnat delays axonal degeneration caused by mitochondrial and oxidative stress. J. Neurosci. 28, 4861–4871.

Ritchie, J.M., 1967. The oxygen consumption of mammalian non-myelinated nerve fibres at rest and during activity. J. Physiol. 188, 309–329.

Ryu, B.R., Jain, R.K., Gonzales, E.R., Lee, J.M., Goldberg, M.P., 2006. Reduction of ischemic axonal degeneration in wlds mice (Abstract). Program No. 177.11. 2006 Neuroscience Meeting Planner. Society for Neuroscience, Atlanta, GA (Online).

Sajadi, A., Schneider, B.L., Aebischer, P., 2004. Wlds-mediated protection of dopaminergic fibers in an animal model of Parkinson disease. Curr. Biol. 14, 326–330.

Sasaki, Y., Araki, T., Milbrandt, J., 2006. Stimulation of nicotinamide adenine dinucleotide biosynthetic pathways delays axonal degeneration after axotomy. J. Neurosci. 26, 8484–8491.

Sasaki, Y., Vohra, B.P., Lund, F.E., Milbrandt, J., 2009. Nicotinamide mononucleotide adenylyl transferase-mediated axonal protection requires enzymatic activity but not increased levels of neuronal nicotinamide adenine dinucleotide. J. Neurosci. 29, 5525–5535.

Saxton, W.M., Hollenbeck, P.J., 2012. The axonal transport of mitochondria. J. Cell Sci. 125, 2095–2104.

Schlaepfer, W.W., Bunge, R.P., 1973. Effects of calcium ion concentration on the degeneration of amputated axons in tissue culture. J. Cell Biol. 59, 456–470.

Schlaepfer, W.W., Lee, C., Lee, V.M., Zimmerman, U.J., 1985. An immunoblot study of neurofilament degradation in situ and during calcium-activated proteolysis. J. Neurochem. 44, 502–509.

Schweiger, M., Hennig, K., Lerner, F., Niere, M., Hirsch-Kauffmann, M., Specht, T., Weise, C., Oei, S.L., Ziegler, M., 2001. Characterization of recombinant human nicotinamide mononucleotide adenylyl transferase (NMNAT), a nuclear enzyme essential for NAD synthesis. FEBS Lett. 492, 95–100.

Shen, H., Goldberg, M.P., 2012. Creatine pretreatment protects cortical axons from energy depletion in vitro. Neurobiol. Dis. 47, 184–193.

Stys, P.K., 2004. White matter injury mechanisms. Curr. Mol. Med. 4, 113–130.

Stys, P.K., 2005. General mechanisms of axonal damage and its prevention. J. Neurol. Sci. 233, 3–13.

Tolkovsky, A.M., Suidan, H.S., 1987. Adenosine 5′-triphosphate synthesis and metabolism localized in neurites of cultured sympathetic neurons. Neuroscience 23, 1133–1142.

Trapp, B.D., Stys, P.K., 2009. Virtual hypoxia and chronic necrosis of demyelinated axons in multiple sclerosis. Lancet Neurol. 8, 280–291.

Underhill, S.M., Goldberg, M.P., 2007. Hypoxic injury of isolated axons is independent of ionotropic glutamate receptors. Neurobiol. Dis. 25, 284–290.

Wang, X., Schwarz, T.L., 2009. The mechanism of Ca^{2+}-dependent regulation of kinesin-mediated mitochondrial motility. Cell 136, 163–174.

Wang, J., Zhai, Q., Chen, Y., Lin, E., Gu, W., McBurney, M.W., et al., 2005. A local mechanism mediates NAD-dependent protection of axon degeneration. J. Cell Biol. 170, 349–355.

Waxman, S.G., 2006. Ions, energy and axonal injury: towards a molecular neurology of multiple sclerosis. Trends Mol. Med. 12, 192–195.

Yager, J.Y., Brucklacher, R.M., Vannucci, R.C., 1991. Cerebral oxidative metabolism and redox state during hypoxia-ischemia and early recovery in immature rats. Am. J. Physiol. 261, H1102–H1108.

Yahata, N., Yuasa, S., Araki, T., 2009. Nicotinamide mononucleotide adenylyltransferase expression in mitochondrial matrix delays Wallerian degeneration. J. Neurosci. 29, 6276–6284.

Yang, H., Yang, T., Baur, J.A., Perez, E., Matsui, T., Carmona, J.J., et al., 2007. Nutrient-sensitive mitochondrial NAD^+ levels dictate cell survival. Cell 130, 1095–1107.

Yi, M., Weaver, D., Hajnóczky, G., 2004. Control of mitochondrial motility and distribution by the calcium signal: a homeostatic circuit. J. Cell Biol. 167, 661–672.

Zhai, Q., Wang, J., Kim, A., Liu, Q., Watts, R., Hoopfer, E., et al., 2003. Involvement of the ubiquitin-proteasome system in the early stages of Wallerian degeneration. Neuron 39, 217–225.